Eur. Phys. J. D **16**, 133–138 (2001)

THE EUROPEAN
PHYSICAL JOURNAL D
EDP Sciences

Theoretical exploration of ultrafast spectroscopy of small clusters

V. Bonačić-Koutecký[1,a], M. Hartmann[1], and J. Pittner[2]

[1] Walther-Nernst-Institut für Physikalische und Theoretische Chemie, Humboldt-Universität zu Berlin, Bunsenstraße 1, 10117 Berlin, Germany
[2] J. Heyrovský Institute of Physical Chemistry, Academy of Sciences of the Czech Republic, Dolejškova 3, CZ-18223 Prague

Received 22 December 2000

Abstract. We present the ultrafast multistate nuclear dynamics involving adiabatic and nonadiabatic excited states of non-stoichiometric halide deficient clusters ($\mathrm{Na}_n\mathrm{F}_{n-1}$) characterized by strong ionic bonding and one-excess electron for which the "frozen ionic bonds" approximation has been justified allowing to consider the optical response of the single excess electron in the effective field of the other electrons. We combined the Wigner-Moyal representation of the vibronic density matrix with the *ab initio* multi state molecular dynamics in the ground and excited electronic states including the nonadiabatic couplings calculated "on the fly" at low computational demand. This method allows the simulation of femtosecond pump-probe and pump-dump signals based on an analytical formulation, which utilizes temperature dependent ground state initial conditions, an ensemble of trajectories carried out on the electronic excited state as well as on the ground state after the passage through the conical intersection in the case of nonadiabatic dynamics and for probing either in the cationic state or in the ground state. The choice of the systems we presented has been made in order to determine the timescales of the fast geometric relaxation leaving the bonding frame intact as during the dynamics in the first excited state of $\mathrm{Na}_4\mathrm{F}_3$, and of the bond breaking processes leading to conical intersection between the first excited state and the ground state as in $\mathrm{Na}_3\mathrm{F}_2$. The former is the smallest finite system prototype for an surface F-center of bulk color centers. The latter allows to study the photo isomerization in full complexity taking into account all degrees of freedom. In the case of $\mathrm{Na}_4\mathrm{F}_3$ after the fast geometric relaxation in the excited state leading to deformed cuboidal structure without breaking of bonds, different types of internal vibrational redistribution (IVR) processes have been identified in pump-dump signals by tuning the dump laser. In contrast, from the analysis of the pump-probe signals of $\mathrm{Na}_3\mathrm{F}_2$ cluster, the timescales for the metallic and the ionic bond breaking, as well as for the passage through conical intersection have been determined. Finally the conditions under which these processes can be experimentally observed have been identified.

PACS. 31.15.Qg Molecular dynamics and other numerical methods – 71.15.Qe Excited states: methodology

1 Introduction

Due to remarkable advances in femtosecond spectroscopy involving different laser techniques [1], the need for the theory and simulations became apparent, since they provide the conceptual framework of the ultrafast dynamics. This occurs by characterizing the nature of configurational changes and IVR in vertically excited or ionized states of molecules and clusters [2]. In this context clusters offer the possibility to investigate different processes as a function of their size and degrees of freedom [3]. We wish to emphasize that the basic requirement for the study of intracluster multistate nuclear dynamics in fs-spectroscopy, involving generation of initial conditions, the systems itself and the probe or dump step is the use of accurate ground and excited electronic states including the nonadiabatic couplings, if necessary, as function of all degrees of freedom. The accurate precalculated *ab initio* energy surfaces have been limited to only few degrees of freedom. Therefore, in order to develop theoretical approaches to fs-spectroscopy for systems with moderate number of degrees of freedom, the methods for the MD "on the fly" not only for the ground but also for excited states, and moreover at low computational demand, are requested.

We wish to point out that our *ab initio* approach to molecular dynamics "on the fly" involving excited states of non-stoichiometric halide deficient clusters ($\mathrm{Na}_n\mathrm{F}_{n-1}$) based on the "frozen ionic bonds" approximation should be viewed as starting point of the future development [4,5]. Moreover, it is fortuitous that $\mathrm{Na}_n\mathrm{F}_{n-1}$ clusters with the single excess electron localized either in the vacancy due to the halide deficiency ($\mathrm{Na}_4\mathrm{F}_3$) or on alkali atom attached to the ionic subunit ($\mathrm{Na}_3\mathrm{F}_2$) exhibit not only a strong absorption in visible – infrared energy interval [6] for which "frozen ionic bonds" approximation provides accurate description of excited states, but dynamics in the

---

[a] e-mail: `vbk@chemie.hu-berlin.de`

first electronic state of each cluster in this series involves different interesting processes.

In this contribution we address an adiabatic and nonadiabatic approach to the dynamics of the first excited states of Na_4F_3 and Na_3F_2 clusters, [4,5] respectively. In Section 2 we outline the method. Optical and structural properties of the ground and excited states for two selected examples, Na_4F_3 and Na_3F_2, are given in Section 3. The study of Na_4F_3 presented in Section 4 offers opportunity to analyze adiabatic dynamics involving determination of timescales of geometric relaxation in electronic excited state *versus* different types of IVR. In Section 5 we show that the mechanism of photoisomerization at a conical intersection occurs by breaking of ionic and/or metallic bonds in Na_3F_2. Section 6 contains concluding remarks and outlook.

2 Methods

In this section we outline the basic components of our *ab initio* Wigner distribution approach which involves combination of the *ab initio* MD "on the fly" in the framework of the "frozen ionic bonds" approximation and the Wigner-Moyal representation of the vibronic density matrix allowing the simulation of fs pump-probe or pump-dump signals. Since an excellent agreement between description of absorption spectra for Na_4F_3 and Na_3F_2 obtained from MRCI method correlating all electrons and those obtained from "frozen ionic bonds" approximation was achieved (*cf.* Refs. [4,5]), but at substantially lower computational cost for the latter, we formulated in the framework of this model also analytic gradients in the electronic excited states and nonadiabatic couplings in order to carry out the MD "on the fly". This was relatively easy to do because we realized that solution of the "extended" general restricted open-shell coupled perturbed Hartree-Fock equations (CPHF) are needed which are related to the analytic second derivatives of the restricted open shell Hartree-Fock energy. For derivation *cf.* Refs. [4] and [5]. Once the analytic gradient of the one-excess electron energy has been derived, the velocity Verlet time propagation algorithm can be employed to solve equations of motion and to compute the classical trajectories of the nuclei in the adiabatic electronic excited states. Similarly, the implementation of simple analytic expressions derived for nonadiabatic couplings allowed to carry out nonadiabatic dynamics at low computational demand (*cf.* Ref. [5]). In this case we combine the analytic formulation of gradients and nonadiabatic couplings with the molecular dynamics with quantum transitions (MDQT) based on Tully's stochastic fewest switches algorithm [7], which requires a simultaneous solving of the time dependent Schrödinger equation for the one-excess electron and classical equation of motion for the nuclei. Advantages and disadvantages in the MDQT approach are extensively discussed in the literature [8].

Our approach for the calculation of signals involving multistate adiabatic or nonadiabatic dynamics is based on the semiclassical limit of the multi state Wigner-Moyal representation for the vibronic density matrix. For this purpose two approximations have to be introduced in the quantum mechanical Liouville equation for the vibronic density matrix. Only the terms in lowest order in $\hbar$ are retained in the Wigner-Moyal expansion introducing classical trajectories, and the first order truncation of the expansion with respect to the field $E(t)$ restricts the validity of the approach for low field intensities. From the equations of motion for the Wigner distributions, the densities in the excited state (pump step) as well as in the detection state (probing step) can be straightforwardly calculated. The detection state can be either the cationic ground state in the case of NeExPo pump-probe spectroscopy or the neutral ground state for NeExNe pump-dump spectroscopy.

In general, the fs signal is determined by the total occupation of the detection state $S = \lim_{t\to\infty} P_{det}(t)$ where the following expression involving electronic excited states without as well as in the presence of conical intersections has been derived:

$$S[t_d] \sim \int d\mathbf{q}_0 d\mathbf{p}_0 \int_0^\infty d\tau_1 \exp\left\{-\frac{(\tau_1 - t_d)^2}{\sigma_{pu}^2 + \sigma_{pr}^2}\right\} \\ \times \frac{1}{N_{hop}} \sum_{\nu=1}^{N_{hop}} \exp\left\{-\frac{\sigma_{pr}^2}{\hbar^2}[E_{det} - V_{det,x}(\mathbf{q}_x^\nu(\tau_1;\mathbf{q}_0,\mathbf{p}_0))]^2\right\} \\ \times \exp\left\{-\frac{\sigma_{pu}^2}{\hbar^2}[E_{pu} - V_{pu}(\mathbf{q}_0)]^2\right\} P_{00}(\mathbf{q}_0,\mathbf{p}_0), \quad (1)$$

where Gaussian pulse envelopes has been assumed and $E_{pu,det}$ and $\sigma_{pu,det}$ denote excitation energy and pulse duration of the pump pulse (pu) or the detection pulse (det), respectively. For the initial ground state density P_{00} in the phase space of coordinates $\mathbf{q}_0$ and momenta $\mathbf{p}_0$ we assume the Wigner distribution of a canonical ensemble in each of the normal modes which allows to include temperature effects in correspondence with the experimental situations and to take into account the quantum effects of the initial ensemble at low temperatures. The initial conditions for classical trajectory simulations are obtained by sampling this distribution function. According to expression (1) the initial ensemble is promoted to the excited state. The corresponding Franck-Condon transition probability is given by the last exponential determined by the gap V_{pu} between the excited and the ground electronic state. In the case of a nonadiabatic dynamics through conical intersection involving the electronic ground and first excited state, the propagation of the ensemble starts at the excited state but may hop to the ground state according to the fewest switches hopping algorithm. Therefore we denote the coordinates of the propagated state by $\mathbf{q}_x^\nu$ where x is either the excited or the ground state which is determined by the hopping procedure and ν numerates the set of random numbers used in the hopping algorithm. The probe step described by the second exponential consequently includes the average over the number of hoppings N_{hop} where $V_{det,x}$ is the energy gap between the detection state and the propagated state x. The time resolution of the signal is given by the first exponential where t_d

denotes the time delay between the pulses. As it is required in the Wigner distribution approach, an ensemble average over the initial conditions have to be performed. Expression (1) simplifies if only adiabatic dynamics on the excited electronic state is involved. In this case N_{hop}=1 and the propagated state x is equal to the excited state. The application to the investigation of adiabatic dynamics in the framework of NeExNe pump-dump spectroscopy of Na_4F_3 is described in Section 4. The simulated NeExPo pump-probe signals involving nonadiabatic dynamics will be shown for the example of Na_3F_2 in Section 5.

3 Structural and optical properties of Na_4F_3 and Na_3F_2 clusters

The excited states of non-stoichiometric Na_nF_{n-1} clusters arise from excitations of the one-excess electron which is placed in a large energy gap between occupied and unoccupied one-electron levels in analogy to the "valence" and the "conductivity" bands in infinite systems (*cf.* Ref. [6]). The optically allowed transitions for the stable cuboidal structure of Na_4F_3 with the excess electron localized at the corner defect and for both isomers of Na_3F_2 with the C_s (isomer I) and C_{2v} (isomer II) structures are shown in Fig. 1. The absorption spectra for the most stable structures of Na_nF_{n-1} are characterized by the common feature which is the intense transition located in infrared-visible energy [6]. In contrast, the configurational relaxation in the first excited states of these clusters is of completely different nature and therefore diverse dynamical processes are expected as it will be shown in Sections 5 and 6.

The geometric relaxation in the first excited state of Na_4F_3 towards the minimum with an "open cage" structure related to the cuboidal equilibrium geometry leads to the lowering of energy, but the energy gap between the ground and the first excited state minimum remains relatively large (0.6 eV) (*cf.* Fig. 2) because no bond breaking occurs. In other words due to very localized electronic excitation in the first excited state of Na_4F_3 the cuboidal structure with the corner defect deforms but remains intact.

The situation is completely different for Na_3F_2. After the vertical transition at the geometry of the isomer I (Fig. 1) the geometric relaxation in the first excited state involves Na-Na bond breaking leading to the first local minimum of the excited state with small lowering of the energy, but the relaxation proceeds to the absolute minimum with linear geometry $Na-F-Na-F-Na$ corresponding to the conical intersection for which a further substantial decrease of energy occurs due to breaking of an ionic bond. The linear geometry of the conical intersection is also reached after vertical transition to the first excited state at the geometry of the second isomer with the C_{2v} structure (*cf.* Fig. 1).

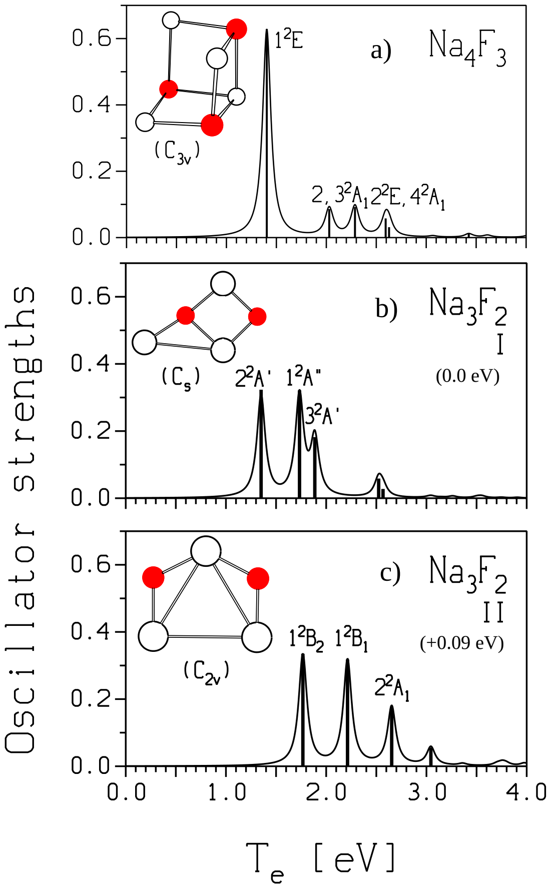

Fig. 1. Optically allowed transitions T_e in eV and oscillator strength f_e obtained from the one-electron "frozen ionic bonds" approximation for the stable ground state structure of Na_4F_3 and for both isomers of Na_3F_2 clusters.

4 Fs-pump-dump signals of Na_4F_3 involving adiabatic dynamic in the excited state

The energetic pump-dump scheme for Na_4F_3 shown in Fig. 2 provides suitable situation for monitoring the ultrafast processes involved in the first excited state of Na_4F_3, since the laser can be tuned starting from 1.4 eV in the Frank-Condon region (cuboidal structure A) to the smallest energy gap of 0.4 eV (strongly distorted cage C) between the ground and excited state, including the energy gap of 0.6 eV corresponding to the minimum of excited state (for the open cage structure B). The thermal ensemble with an initial temperature of 30 K have been assumed. For the characterization of the ensemble dynamics we show in Fig. 3 the energy gaps between the first excited electronic state and the ground state which are characterized by periodic change of gaps. These are due to the strong excitation of the cage opening mode with minima corresponding to C structure and maxima to cuboidal A structure. Beyond 1 ps the periodicity becomes distorted due to restricted IVR process. Therefore, the signals shown on the lower part of Fig. 3 reflect, in addition to the structural relaxation, restricted IVR process

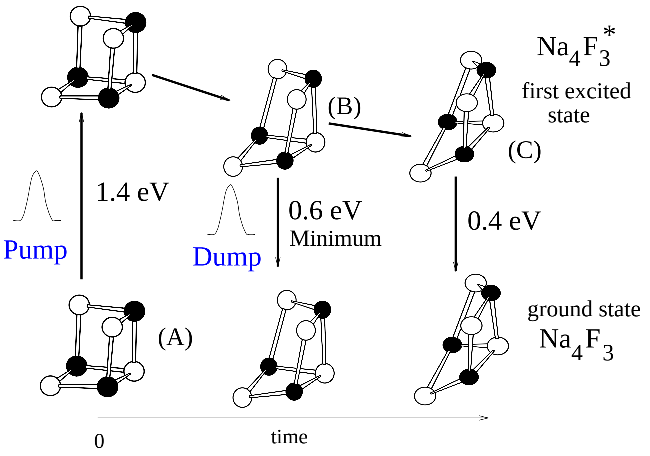

Fig. 2. Pump-dump scheme of the multi state fs dynamics of Na$_4$F$_3$. The dynamics on the first excited electronic state from the initially cuboidal geometry (A) towards the minimum energy "open cage" geometry (B) and continuing to the even more deformed open structure (C) back to the ground state is indicated by thick arrows.

connected with energy loss or energy gain in particular modes.

The simulation of the pump-dump signals using Eq. (1) have been carried out for three different excitation energies of the dump laser (*cf.* Fig. 3b): i) $E_{du} = 1.2$ eV is close to the vertical transition energy corresponding to the cuboidal structure, ii) $E_{du} = 0.6$ eV allows to monitor the dynamics in the minimum of the first excited electronic state, and iii) $E_{du} = 0.8$ eV is an intermediate value which should provide informations about the dynamics connected with the temporal transitions between both the cuboidal and the minimum energy open cage geometry. A dump pulse duration of 100 fs was chosen in order to be able to resolve the structural cage oscillations. The duration between the first maxima of the $E_{du} = 1.2$ eV-signal and the $E_{du} = 0.6$ eV-signal corresponds to the relaxation time from the cuboidal structure to the minimum energy open cage geometry (*cf.* arrows connected with the geometries (A) and (B) in Fig. 3) which is very fast ($\sim$ 100 fs). Furthermore, both the $E_{du} = 1.2$ eV-signal and the $E_{du} = 0.8$ eV-signal exhibit strong oscillations with a period of 260 fs, thus these signals are sensitive to dynamical processes connected with the cage opening mode. In particular, the amplitudes of the maxima of the $E_{du} = 1.2$ eV-signal (*cf.* Fig. 3) are decreasing during the time evolution of the system indicating that the revert to the cuboidal structure is less accomplished from one oscillation period to the other. From the decrease of the signal we can roughly estimate the timescale for this type of one-mode selective IVR of about 1 ps. The "minimum-region" signal ($E_{du} = 0.6$ eV) is aperiodic after 1 ps and the intensity increases significantly indicating that the phase space occupation in the minimum of the first excited electronic state (open cage structure (B) in Fig. 3) raises during the propagation caused by the energy flow into this region. Note that this restricted energy arriving IVR differs from the one-mode selective energy leaving IVR of the cage opening mode since the "minimum-region" signal cannot be attributed to one specific vibrational mode, in contrast to the $E_{du} = 1.2$ eV-signal. Consequently, the timescales of both IVR processes are different. However, as can be seen from Fig. 3, the simulation time of 2 ps is too short in order to determine the timescale for restricted energy arriving IVR. Finally, the average amplitudes of the oscillations of the $E_{du} = 0.8$ eV-signal remain almost constant. This indicates that a somewhat constant part of

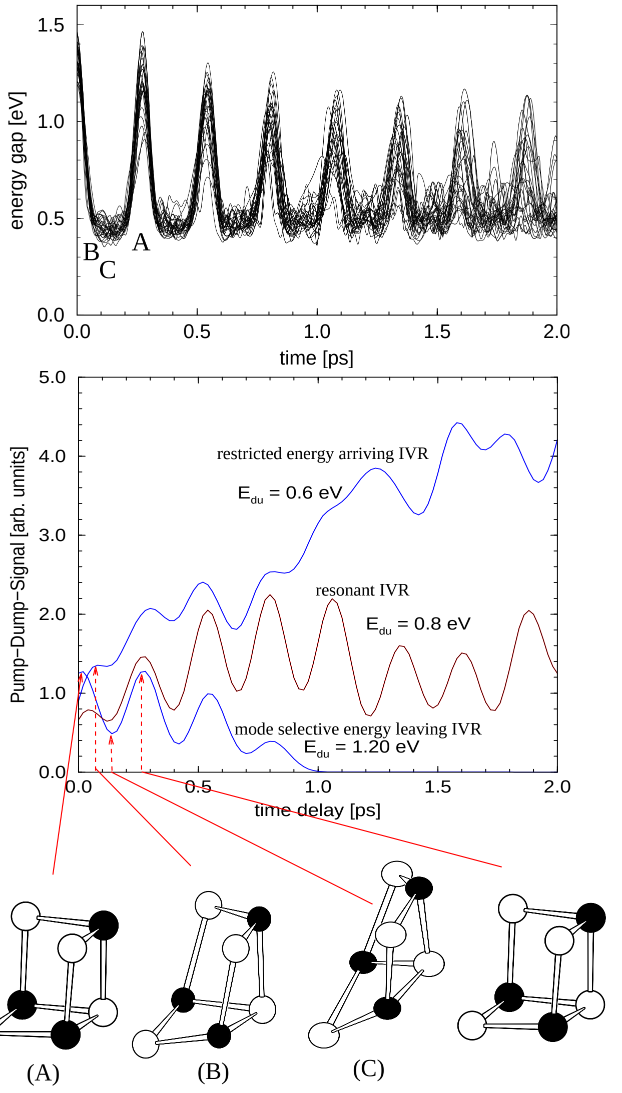

Fig. 3. Bunch of energy gaps between the first excited electronic state and ground state of Na$_4$F$_3$ for 20 representative trajectories during the dynamics on the first excited state obtained for initial temperature of 30 K (upper window). Simulated pump-dump signals at different excess energies of the dump laser. Minima and maxima of the signals indicating the timescales of the structural relaxation process can be attributed to the geometries indicated below; (A) - cuboidal geometry (minimum of the ground state), (B) - "open cage" structure (minimum of the first excited state), (C) - strongly deformed open structure reached due to high vibrational energy. Different types of IVR are indicated (lower window).

the phase space volume oscillates periodically above the minimum structure (B). However, the modulation of the oscillations in the $E_{du} = 0.8$ eV-signal is due to either the anharmonicity of the cage opening mode or resonant IVR which arises from the coupling of the other modes to the still dominant cage opening mode. Finally we want to emphasize that, although the system has fifteen degrees of freedom, no features of dissipative IVR could be found during the propagation time of 2 ps and for low initial temperature. This analysis of the restricted IVR processes can be important for the development of mode selective control mechanisms of these or similar systems with metallic-ionic and metallic-covalent bonds.

5 Fs-pump-probe signals of Na_3F_2 involving nonadiabatic dynamics through conical intersection

We first analyzed the conical intersection using the algorithm introduced by Robb *et al.* [9]. Since the linear geometry of the conical intersection has 10 degrees of freedom, the intersection seam is eight dimensional. The wavefunctions of the ground and the first excited state in the neighborhood of the conical intersection yields positive and negative linear combinations of two "valence bond structures" $Na^+-F^--Na^+-F^--Na\bullet \pm \bullet Na-F^--Na^+-F^--Na^+$, one of them contributing dominantly to the ground and other one to the first excited state, thus giving rise to two states of different symmetry. The location of one-excess electron is indicated by dot above sodium atom (*cf.* Fig. 4). At the conical intersection due to the degeneracy of states any linear combination of the two "VB" structures is possible. These two "VB" structures differ by translocation of the one-excess electron or the positive charge from one and of chain to the other. In analogy to the dissociation limit of H_2^+ molecule the degeneracy between excited and the ground state occurs due to equal energies of $\bullet H-H^+$ and $^+H-H\bullet$ structures which means that the linear chain of Na_3F_2 is sufficiently long to minimize the repulsion between two states and to close the energy gap between them. Therefore, the finding of mechanism for occurrence of conical intersection in Na_3F_2 is of general importance because the analogic electronic situation can be designed and found for other systems as well.

The pump-probe scheme is convenient for the investigation of ultrafast photochemical processes on the first excited state of Na_3F_2 clusters involving the passage through the conical intersection since a second ionizing probe pulls with excitation energies between ~ 2.9 eV and ~ 4.8 eV can be used to monitor the relaxation dynamics in excited state before conical intersection and in ground state after passage through the conical intersection, respectively. The initial conditions have been determined by sampling the Wigner distribution function based on canonical thermal ensemble of 50 K around the energy minimum of the C_s structure.

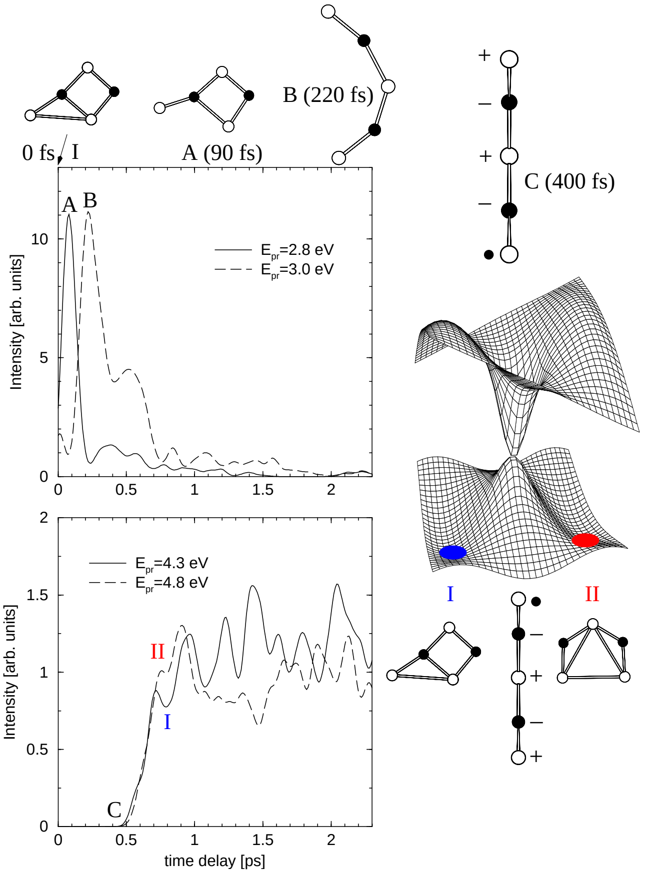

Fig. 4. Simulated pump-probe signals for the 50 K initial temperature Na_3F_2 ensemble at different excitation energies of the probe laser allowing to monitor geometric relaxation on the first excited state involving bond breaking processes (A and B) and passage through the conical intersection (C) (upper windows) as well as geometric relaxation and IVR processes on the ground state after the passage (lower window). A sketch of the conical intersection separating two isomers I and II together with the two "valence bond" structures characterizing the wavefunctions are shown on the right.

The pump-probe signals have been simulated according to equation (1) using energy gaps obtained from the classical trajectory simulations based on the fewest switching hopping algorithm for the ensemble of 50 K initial temperature. Zero pump pulse duration ($\sigma_{pu} = 0$) involving a complete excitation of the ground state ensemble prepared at the initial temperature was assumed. However, a probe pulse duration of 50 fs was chosen which allows to resolve the ultrafast structural relaxation processes involving the bond breaking. The simulations of the signals have been performed for four different excitation energies (wavelengths) of the probe pulse: i) $E_{pr} = 2.8$ eV and $E_{pr} = 3.0$ eV correspond to transition energy values between the first excited and the cationic state at the time of the Na-Na metallic and the Na-F ionic bond breaking, respectively. Thus the signals for the above transition energies provide the information on the structural relaxation involving the bond breaking processes in the first excited state of Na_3F_2 before the conical intersection is reached.

In fact, they exhibit maxima at ∼ 90 fs and ∼ 220 fs (*cf.* Fig. 4) in agreement with the timescales for the metallic and ionic bond breaking obtained from the analysis of the phase space distribution and energy gap values. Both signal intensities decrease rapidly after 0.4-0.5 ps indicating the branching of the phase space density from the first excited electronic state to the ground state due to the conical intersection. ii) $E_{pr} = 4.3$ eV and $E_{pr} = 4.8$ eV (*cf.* Fig. 4) correspond to transition energies between the ground state and the cationic state at the C_s geometry and the C_{2v} geometry, respectively. In such a way, the signals monitor the ratio of both isomers in the phase space distribution after the passage through the conical intersection up to a time delay between pump and probe of ∼ 1 ps. For larger time delays, the signals provide only informations about the energetic redistribution, thus IVR. In fact, the intensities of both signals start to increase after ∼ 0.4 ps since the ground state becomes populated providing the time scale for the passage through the conical intersection (*cf.* Fig. 4). Furthermore, the signal at $E_{pr} = 4.8$ eV exhibits a maximum at 0.8–0.9 ps indicating the larger ratio of the C_{2v} structure. This signal drops rapidly after 0.9 ps and the signal at $E_{pr} = 4.3$ eV increases indicating that the C_s structure is more populated at 0.9–1.0 ps (*cf.* Fig. 4). The latter one also exhibits oscillatory features beyond 1 ps, *i.e.* corresponding to the IVR regime, which leads to the conclusion that a somewhat periodic energy flow is present in the cluster ensemble. Of course, due to the high vibrational excess energy, these oscillations cannot be attributed to particular normal modes.

These results show that different physical processes are involved in the dynamics of Na_3F_2 cluster initiated by the Frank-Condon pump pulse transition to the first excited electronic state, such as geometric relaxation, consecutive bond breaking of metallic and ionic bonds, passing through the conical intersection, and IVR processes. Moreover, the timescales of these processes can be identified in pump-probe signals and each of them can be selectively monitored by tuning of the probe excitation energy.

6 Summary and outlook

We have presented simulated pump-dump and pump-probe signals based on the *ab initio* adiabatic and non-adiabatic MD "on the fly" involving systems with 15 (Na_4F_3) and with 9 (Na_3F_2) degrees of freedom.

The dynamics on the first excited state of Na_4F_3 represents the prototype of process involving fast geometric relaxation without bond breaking followed by different types of IVR which can be identified by the proper tuning of the dump laser. Moreover, since the dissipative IVR has not been identified for low temperature initial conditions, it is to expect that this will be also the case for large systems with localized defects. This might be of importance for introducing control of mode selectivity in complex systems.

The study of the *ab initio* nonadiabatic dynamics through the conical intersection between the first excited and the ground state of Na_3F_2 has been addressed in full complexity, using combination of different theoretical approaches which has not been accomplished previously. This allowed to determine timescales for breaking of metallic and ionic bonds as well as for isomerization process through the conical intersection. The mechanism of the photo isomerization through a conical intersection in atomic clusters is an important generalization of the processes known in bioorganic photochemistry [10] (*e.g.* cis-trans isomerization of the retinal chromophore in the vision process taking place within ∼ 200 fs). Moreover the experimental identification of isomerization process through conical intersection of Na_3F_2 in the gasphase has a good chance to be realized, since the time scale is sufficiently long (∼ 400 fs). In fact the fs pump-dump and pump-probe experiments are in progress [11].

The aim of the future work is to determine conditions for controlling the photochemical isomerzation process through the conical intersection. Finally we wish to point out that change of the cluster size connected with the different structural properties gives rise to very different dynamical processes on the ultrafast timescale. Furthermore we have shown that theory provides conceptual framework of ultrafast spectroscopy and allows to formulate conditions under which different processes can be experimentally observed.

This work was supported by the "Sonderforschungsbereich 450, Analyse und Steuerung photoinduzierter ultraschneller Reaktionen" of the *Deutsche Forschungsgemeinschaft*. The calculations have been partly carried out at the *Konrad-Zuse-Zentrum für Informationstechnik* Berlin.

References

1. A.H. Zewail, J. Phys. Chem. A **104**, 5660 (2000).
2. M. Hartmann, J. Pittner, V. Bonačić-Koutecký, A. Heidenreich, J. Jortner, J. Chem. Phys. **108**, 3096 (1998); M. Hartmann, A. Heidenreich, J. Pittner, V. Bonačić-Koutecký, J. Jortner, J. Phys. Chem. A **102**, 4069 (1998).
3. J. Jortner, *Femtochemistry*, edited by M. Chergui (World Scientific, Singapore, 1996).
4. M. Hartmann, J. Pittner, V. Bonačić-Koutecký, J. Chem. Phys. **114**, 2106 (2001).
5. M. Hartmann, J. Pittner, V. Bonačić-Koutecký, J. Chem. Phys. **114**, 2123 (2001).
6. V. Bonačić-Koutecký, J. Pittner, J. Koutecký, Chem. Phys. **210**, 313 (1996); V. Bonačić-Koutecký, J. Pittner, Chem. Phys. **225**, 173 (1997).
7. J.C. Tully, J. Chem. Phys. **93**, 1061 (1990).
8. J.-Y. Fang, S. Hammes-Schiffer, J. Phys. Chem. A **103**, 9399 (1999).
9. I.N. Ragazos, M.A. Robb, F. Bernardi, M. Olivucci, Chem. Phys. Lett. **197**, 217 (1992).
10. J. Michl, V. Bonačić-Koutecký, *Electronic Aspects of Organic Photochemsitry* (Wiley, New York, 1990).
11. S. Vajda, L. Wöste, private communication.